Sensorless Terrain Estimation for a Wheeled Mobile Robot

S. D. Arunya P. Senadheera, A. M. Harsha S. Abeykoon
Department of Industrial System Engineering
Asian Institute of Technology
Pathumthani, Thailand
arunyasenadeera@gmail.com, harsha@ait.asia

***Abstract*— Estimating the terrain for a wheeled mobile robot is challenging task when slip information is absent. Most of wheeled mobile robots are using different kinds of sensors to estimate the slip ratio and other surface condition measurements. This paper introduces a simple, yet novel method to estimate the terrain, using rolling resistance torque without using any additional sensors. Reaction torque observer is used to obtain the rolling resistance torque in different terrains. Proposed concept is practically verified by using a differential drive mobile robot.**

Keywords—Rolling Resistance, Wheeled Mobile Robot,Reaction Torque Observer, Disturbance observer, Terrain Estimation

I. INTRODUCTION

Electric Vehicles (EVs) have become dominant in the transportation field over Internal Combustion Vehicles (ICVs). EVs are more attractive than ICVs, because the torque of each wheel can be accurately controlled. Zero emission and energy efficiency are the other most attractive advantages of EVs. Terrain estimation has become an essential feature of the EVs, as it directly affects the vehicle stability, anti-lock braking system (ABS) and the dynamic stability controller. Wheeled Mobile Robot (WMR), which is a scaled down version of a EVs that could be controlled autonomously, semiautonomous or remotely in different terrains. It is more important to estimate the terrain of a WMR, compared to the other vehicles as there is no driver on board to observe and control as for the road conditions.

In ideal conditions, WMR wheels satisfy the condition of pure rolling without slipping in any terrain. Terrain estimation and torque control is essential to achieve maximum traction force. Chen et al. [1] proposed a method to build 3D model of the road surface by using accelerometers, cameras, GPS and Inertial Measurement Units (IMUs). This method involves complex calculations which cannot be used in a small scale micro-controller (like this study) based WMRs. Their sensors occupy more space. Rafael et al. [2] proposed multilayer perceptron neural network to classify the sand, asphalt, grass and soil terrains for a WMR. A 3-axis accelerometer is used as an input sensor to the system. A DSP board is required for the ADC conversion of accelerometer data and an extra effort is required for removing the noises from the accelerometer data. The slip ratio estimation or measurement can be used to estimate the terrain, rather than directly acquiring the data from the sensors.

Abeykoon et al. [3] proposed a non-driven trailing wheel to detect the slip ratio. However, it is not effective, as the slip ratio is become small value when the WMR is moving at a smaller velocity. So, it can't be detected from the trailing wheel. H. Sado et al. [4] used a front wheel driven EV, and rear wheels as the trailing wheels to calculate the slip ratio. In that study, version of DOB (Disturbance Observer), is used to obtain the driving force of the vehicle. The trailing wheels are also slipping in real world application. Therefore, it is not suitable to use trailing wheels to calculate the slip ratio as proposed in [4]. H. Fujimoto et al. [5] proposed a method to use the DOB with an accelerometer to calculate slip ratio of the EVs. The velocity is calculated from the accelerometer data by integrating the acceleration of the vehicle. Errors of the accelerometer data are also integrated with the velocity. Therefore, the velocity of the vehicle cannot be measured from the accelerometer accurately to calculate the slip ratio. LuGre dynamic friction model could be used to estimate the terrain [6]. Y.Chen et al. [7] used GPS to obtain the velocity of the vehicle. The GPS signal is weak in a covered indoor terrain. Y.Chen et al. [7] proposed a system that could be simulated a high performance computer. However, such a system cannot be implemented using a micro-controller.

WMR platforms are frequently used in both indoor and outdoor terrains. Sensors that are used to estimate the terrains are having limitations and ineffective. Therefore, the terrain estimation algorithms that rely on sensors are always vulnerable. This paper proposes a novel but a simple method to estimate the terrain without any additional sensors.

This paper is organized as follows. In Section 2, driven wheel dynamics is explained. Further, the rolling resistance force is described. Then, the Disturbance Observer (DOB) and the Reaction Torque Observer (RTOB) are explained in Section 3. Rolling Torque Observer, Kinematics of WMR and Dynamics of WMR are illustrated in Section 4, Section 5 and Section 6 respectively. The experimental results are shown in Section 7. Finally, the paper is concluded in Section 8.

II. MODELLING

Wheel mobile robot (WMR) which is moving on a flat surface, is governed by the dynamics [8] as shown in (1).

$$M\dot{v}_c = F_x - F_r \tag{1}$$

Where the M is mass of the WMR, v_c is longitudinal velocity, F_x is longitudinal friction force and F_r is the rolling resistance force. Translational motion of the WMR can be integrated with the driven wheel dynamics of the wheels of the robot. A simple model of the driven wheel dynamic is shown in Fig.1. Driven wheel dynamics can be expressed as in (2).

$$\mathcal{I}\ddot{\theta} = T_d - RF_x + RF_r \quad (2)$$

$$v_r = R\dot{\theta} - v_c \quad (3)$$

Where $\mathcal{I}$ is the wheel inertia, $\ddot{\theta}$ is angular acceleration, T_d is driving torque, R is wheel radius and N is normal force.

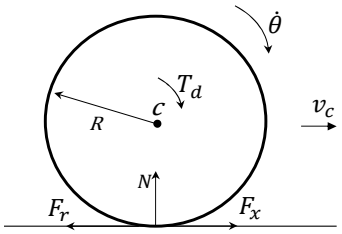

Fig.1. Driven Wheel Dynamics

The WMR's relative velocity v_r can be obtained from (3). The relative velocity generates the tractive force for the wheels from the friction force between the tire and the ground. The coefficient of the friction $\mu_{(\lambda)}$ is a function of the slip ratio. Dynamic friction coefficient has been modelled in the literature by using Lugre model [6], Dagoff model [8] and Magic Formula [8]. The relationship between longitudinal friction force and the normal force can be represented by (4).

$$F_x = \mu_{(\lambda)} N \quad (4)$$

The slip ratio is small and can be neglected when the WMR attains a constant velocity. The rolling resistance force can be considered as the only force that opposed the motion in the low velocities [8]. The air drag force is acting against the motion, after the speed researched to a certain limit. The driving torque can be obtained from (5), when the wheel rotates in constant and low angular velocities. This is equivalent to a pure rolling without slipping.

$$T_d = -RF_r \quad (5)$$

The driving torque can be obtained and measured from the RTOB. The Rolling friction coefficient depends on many factors such as tire temperature, inflation pressure velocity and surface [9]. In low velocities rolling friction coefficient, C_r is assumed to be constant value [9]. Hence, the normal load that is acting on the tire. Pressure and temperature inside the tire are assumed to be constants. However the rolling force is changing as a function of the surface conditions. The relationship between normal load and the rolling resistance force can be expressed as (6).

$$F_r = C_r N \quad (6)$$

III. Disturbance Observer(DOB) and Reaction Torque Observer(RTOB)

A. Disturbance Observer(DOB)

WMRs are constantly exposed to disturbances acting on its wheels. Those unknown disturbances may unstabilize the system if it is not taken into consideration. Ohnishi et al. [10] is proposed a DOB for DC motor control applications to detect and compensate for unknown disturbances that act on the motor. Total disturbance forces that acting on the motor can be obtained from (7). K_{tn} denotes the motor current constant, J_n is the inertia of the motor rotor and the n subscript implies that the nominal values. I_a^{ref} denotes the reference current for the motor. Here $\ddot{\theta}$, the angular acceleration of the motor, which needs to be found from the second derivative of the angular displacement, which is measured from the encoder reading. The DC motor model is shown in Fig.2.

$$T_{dis} = K_{tn} I_a^{ref} - J_n \ddot{\theta} \quad (7)$$

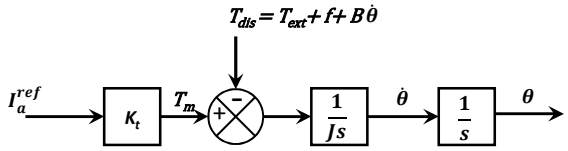

Fig.2.DC motor model

As for the Fig.2, $(f + B\dot{\theta})$ term denotes the sum of the static friction and viscous friction, where B is viscous friction coefficient and $\dot{\theta}$ is the angular velocity of the motor. T_{ext} is the external toque that exerted on motor shaft. Disturbance Observer block diagram is shown in Fig.3. K_t and J are the actual motor current constant and actual motor rotor inertia respectively. $\hat{\tau}$ is the estimated disturbance toque from disturbance observer. G_{dis} denotes the first order low-pass filter cutoff frequency of the software filter.

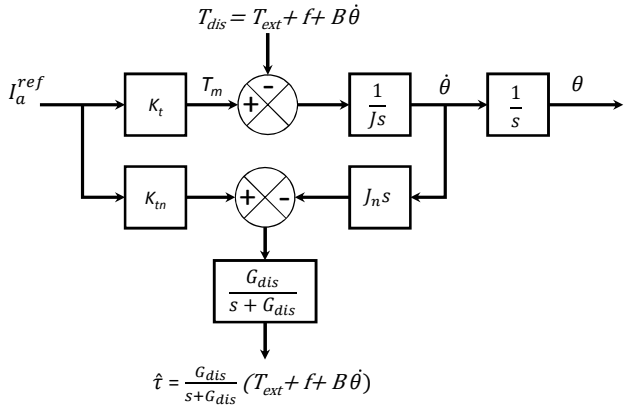

Fig.3.Block diagram of the DOB

B. Reaction Torque Observer(RTOB)

When WMR is moving at a constant velocity, RTOB is used to observe the rolling resistance torque on both wheels. The RTOB block diagram is shown from Fig. 4.

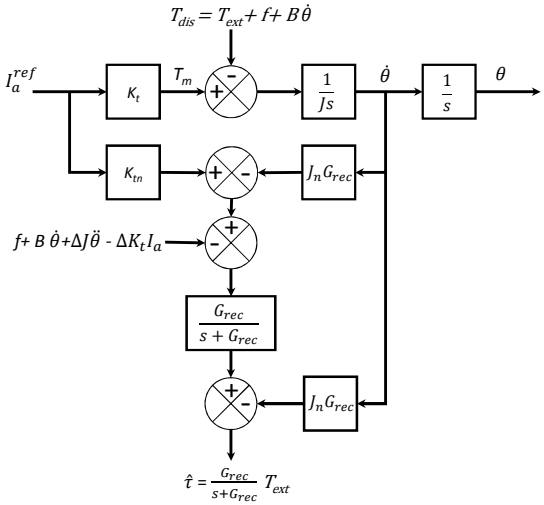

Fig.4.Block diagram of the RTOB

ΔK_t and ΔJ denote the parameter variations or the measurement errors of the K_t and J. G_{rec} denotes the first order low-pass filter cutoff frequency in the software filter.

IV. Rolling Torque Observer

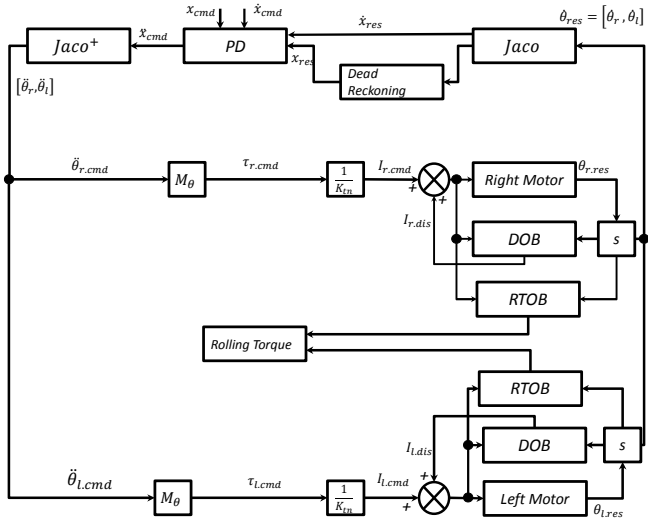

Fig.5.Block diagram of Rolling Torque Observer

Proposed control algorithm block diagram is shown in Fig.5. The commanded path and velocities are predefined. WMR is commanded to move on polished cement, rubber carpet and tar road. The rolling torque of the wheels can be obtained from the RTOB. Rolling torque is analyzed to estimate the terrain when WMR is moving on a straight path with a constant linear velocity. When the WMR is moving on a curved path, right and left wheels are experiencing different torque profiles depending on the path it follows. Therefore, the terrain estimation has to be done during the straight movements.

V. Kinematics of the WMR

The position and velocity commands are with respect to the world coordinate system. So, it is needed to have a transformation matrix, which converts the angular velocities and displacements to the world coordinate system. The kinematic model is shown in Fig.6. Here R is the radius of the wheel and W is width of the WMR.

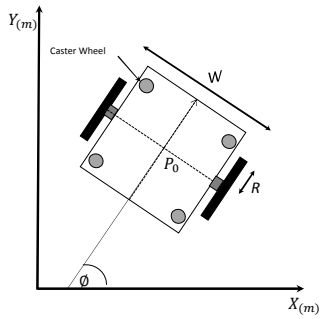

Fig.6. The Kinematics model of WMR in world coordinate system

As for the Fig.6, Po is the middle point of the WMR. The WMR position and orientation can be expressed as in (8). It is defined in the world coordinate system by using x(x-coordinate), y(y-coordinate) and the attitude angle $\emptyset$.The angular displacement of right and left wheels is denoting by θ_r, θ_l respectively as shown in (9).

$$X = [x \quad y \quad \emptyset]^T \tag{8}$$

$$\theta = [\theta_r \quad \theta_l]^T \tag{9}$$

The direct kinematic equation can be represented from (10), where the Jacobean matrix is shown in (11).

$$\begin{bmatrix} \dot{x} \\ \dot{y} \\ \dot{\emptyset} \end{bmatrix} = \begin{bmatrix} \frac{R\cos\phi}{2} & \frac{R\cos\phi}{2} \\ \frac{R\sin\phi}{2} & \frac{R\sin\phi}{2} \\ \frac{R}{W} & -\frac{R}{W} \end{bmatrix} \begin{bmatrix} \dot{\theta}_r \\ \dot{\theta}_l \end{bmatrix} \tag{10}$$

$$J_{aco} = \begin{bmatrix} \frac{R\cos\phi}{2} & \frac{R\cos\phi}{2} \\ \frac{R\sin\phi}{2} & \frac{R\sin\phi}{2} \\ \frac{R}{W} & -\frac{R}{W} \end{bmatrix} \tag{11}$$

It is needed to calculate the inverse kinematic equation from the direct kinematic equation as shown in (12). The pseudo inverse matrix J_{aco}^+ need to be used, because Jacobean matrix is not square matrix. Inverse kinematic equation is differentiated and can be obtained as shown in (13). It can be assumed that $\dot{J}_{aco}^+$tends to zero as shown in (14), because the ϕ is not changing rapidly and R/W is a constant value.

$$\dot{\theta} = J_{aco}^+ \dot{X} \tag{12}$$

$$\ddot{\theta} = \dot{J}_{aco}^+ \dot{X} + J_{aco}^+ \ddot{X} \tag{13}$$

$$\ddot{\theta} = J_{aco}^{+}\ddot{X} \tag{14}$$

J_{aco}^{+}can be denoted as,

$$J_{aco}^{+} = \frac{1}{R}\begin{bmatrix} cos\emptyset & sin\emptyset & \frac{W}{2} \\ cos\emptyset & sin\emptyset & \frac{W}{2} \end{bmatrix} \tag{15}$$

A. Dead-Reckoning

Dead-Reckoning is used to estimate the *x*,*y* positions and attitude angle of the WMR that can be expressed from (16), (17) and (18) respectively.

$$x_k = x_{k-1} + v.cos\left(\frac{\emptyset_k + \emptyset_{k-1}}{2}\right).\Delta t \tag{16}$$

$$y_k = y_{k-1} + v.sin\left(\frac{\emptyset_k + \emptyset_{k-1}}{2}\right).\Delta t \tag{17}$$

$$\emptyset = \frac{R}{W}(\theta_r - \theta_l) \tag{18}$$

In (16) and (17) subscript *k* denote the values at time *k*. The subscript *k-1*denotes values at *k-1*. Here v is the velocity in the world coordinate system. Δt denotes the sampling time.

VI. Dynamics of the WMR

Torque of the left and right wheels can be denoted as (19) .

$$\begin{bmatrix} \tau_r \\ \tau_l \end{bmatrix} = M_\theta.R^2.\begin{bmatrix} \ddot{\theta}_r \\ \ddot{\theta}_l \end{bmatrix} \tag{19}$$

Where inertia matrix,M_θ denotes as (20),

$$M_\theta = \begin{bmatrix} \frac{M}{4} + \frac{J}{W^2} + \frac{J_w}{R^2} & \frac{M}{4} - \frac{J}{W^2} \\ \frac{M}{4} - \frac{J}{W^2} & \frac{M}{4} + \frac{J}{W^2} + \frac{J_w}{R^2} \end{bmatrix} \tag{20}$$

In (20), *M* is the mass of the WMR, *J* is the Inertia of the WMR around an axis vertical to the *x*-*y* plane and J_w is inertia of each wheel.

VII. Results

A differential drive mobile robot is used for this research study. Closed loop current controlled motor drivers are used to run the DC motors. Each wheel is attached with a 400PPR incremental rotary encoder. The WMR is shown in Fig.7. STM32F429 Discovery development board is programmed to run at 500 µs sampling time with a Real-Time Operating System (RTOS). Data is recorded to a microSD card that communicated over SPI protocol. GNUPLOT software is used to plot graphs.

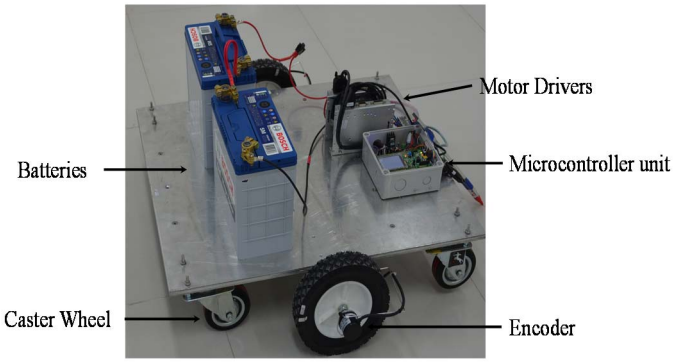

Fig.7: WMR used for research

Different test runs are carried out in different terrains (tar road, polished cement and Rubber carpet) with different speeds (0.05, 0.1, 0.2, 0.3, 0.4, 0.5, 0.6 m/s).Then RTOB output is recorded. The RTOB output includes any kind of wheel eccentrics, motor eccentrics and any longitudinal forces that are appeared in the wheels. A 10-meter straight line path is commanded to keep the constant velocity, in different terrains. RTOB output mean was recorded when the WMR has achieved the constant velocity.

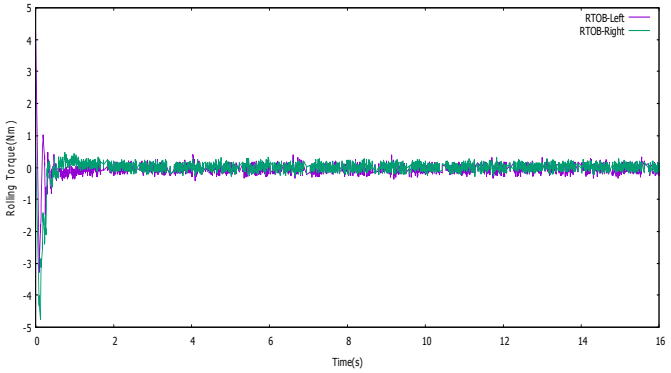

Fig.8: Rolling torque for freewheel of WMR

The RTOB output represents various frictional components (coulomb and viscous friction) of the system and the driving torque of the WMR. The friction components are experimentally found out and compensated at the system. Then the RTOB corrected output shows the driving torque of WMR. The RTOB output is expected to show zero, when the wheels are freely rotating. As in Fig.8 the RTOB output, when the WMR wheels are freely rotating. Fig.9 and Fig.10 represent the typical position response and longitudinal velocity of the WMR respectively.

The RTOB output in the polished cement floor with the longitudinal velocity of 0.1 m/s is shown in Fig.11.The RTOB output needs to be a constant value throughout the constant velocity period. However, the output is appeared as a sinusoidal function, as the wheels have eccentrics.

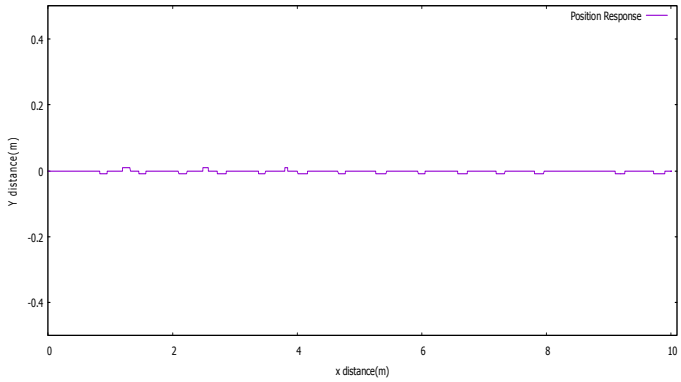

Fig.9: Typical position response of WMR

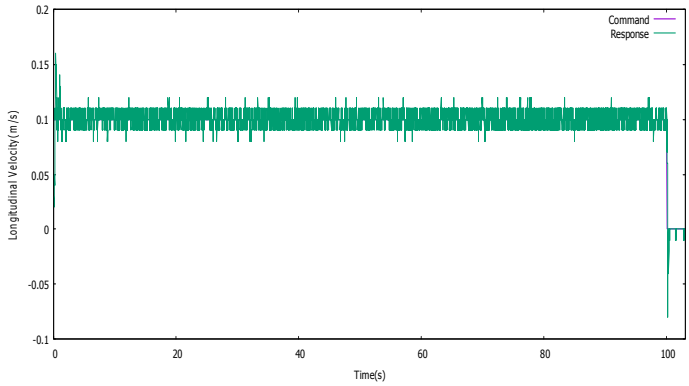

Fig.10: 0.1 m/s Longitudinal velocity profile of WMR

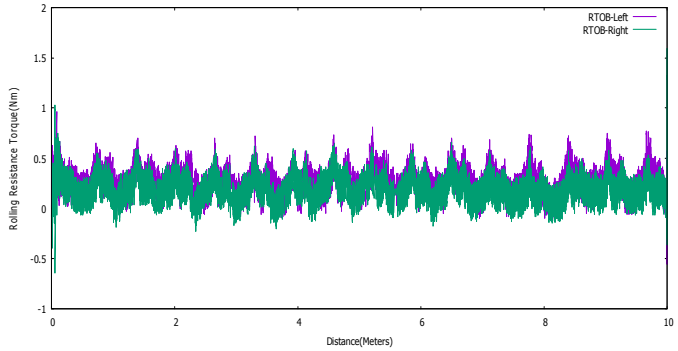

Fig.11: RTOB output in polished cement floor

Many tests were conducted to find out the relationship between rolling resistance force and the WMR longitudinal velocity. The rolling resistance torque's mean is plotted against the longitudinal velocity of the WMR. It is shown in Fig.12. The rolling resistance torque is almost a constant value in low velocities, which could be seen from the plot. Similarly, tests are performed on a rubber carpet and on a tar road to obtain the rolling resistance torques.

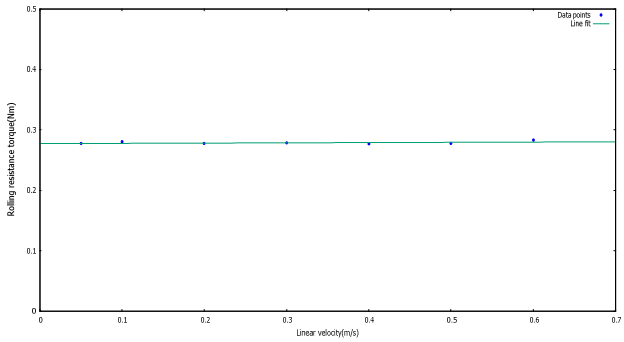

Fig.12: Line fit to rolling resistance torque mean on polished cement

Fig.13 is shows the WMR moved over two surfaces. The rolling resistance force is varied with the surface. This feature could be used to estimate the terrain. Rolling resistance torque's mean values on different terrains is shown in Fig. 14.

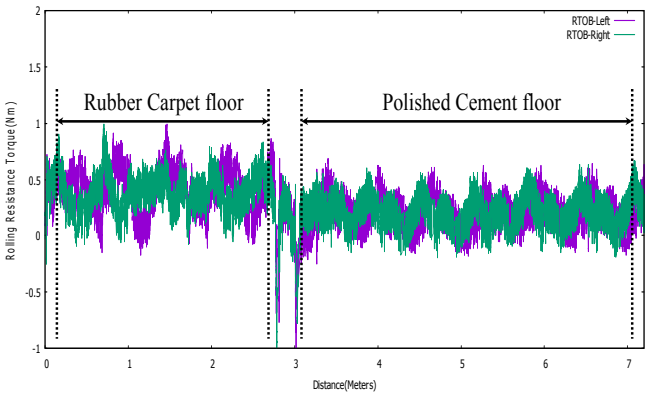

Fig.13: WMR went over two surfaces

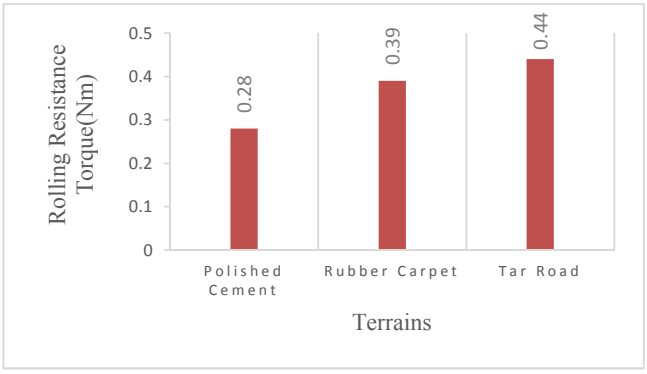

Fig.14: Rolling resistance torque on different surfaces

RTOB output is further analyzed with a Box and Whisker plot. Box and Whisker plot is shown in Fig.15. As for the results, the rolling resistance torques could be used to detect the terrain conditions.

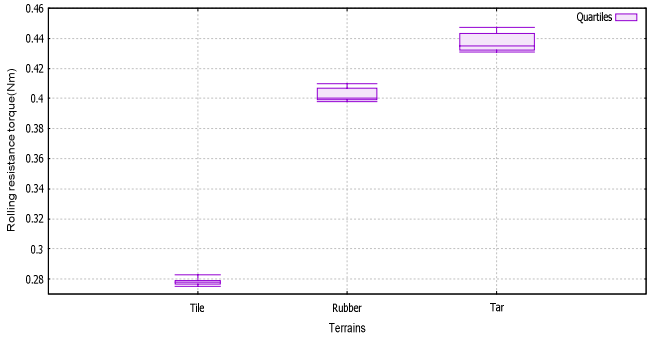

Fig.15: Box and Whisker plot of RTOB data

Fast Fourier Transform (FFT) also can be used to estimate the indoor and outdoor terrains. The FFT of Polished cement and Tar road are shown in Fig.16 and Fig.17 respectively. Terrain is estimated by analyzing the 3dB point, cutoff frequency in each plot. Test results are confirmed that 3db cutoff do not change with the velocity for the given terrain. Table 1 tabulats the 3dB cutoff frequency in Tar road and polished cement surfaces.

Surface	**3dB cutoff frequency(Hz)**
Tar Road	0.7
Polished Cement	4.0

Table 1: 3dB cutoff for indoor and outdoor terrains

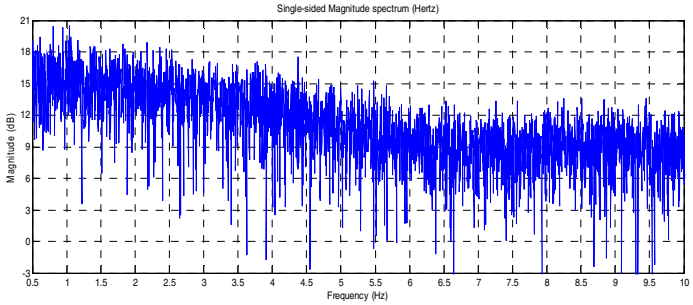

Fig.16: FFT of the RTOB output on polished cement

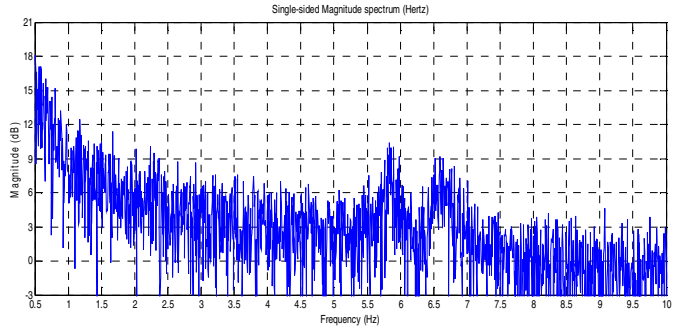

Fig.17: FFT of the RTOB output on Tar road

VIII. Conclusions

This paper, proposed a novel, yet a simple method to estimate the terrains for WMRs. In this study, no additional sensors are used. RTOB is used to measure the rolling resistance torque. The frictional components are experimentally found and compensated at the RTOB. The proposed method of terrain estimation is validated experimentally for a differential drive robot. Proposed method is suitable to be used in EVs. This method could be used to detect wheel eccentrics in WMRs or EVs as well. Accuracy of the proposed method could be enhanced by reducing the wheel and motor eccentrics.

References

[1] Y. L. Chen *et al.*, "Inexpensive Multimodal Sensor Fusion System for Autonomous Data Acquisition of Road Surface Conditions," in *IEEE Sensors Journal*, vol. 16, no. 21, pp. 7731-7743, Nov.1, 2016.

[2] R. Tolentino-Rabelo and D. M. Muñoz, "Online terrain classification for mobile robots using FPGAs," *2016 IEEE 7th Latin American Symposium on Circuits & Systems (LASCAS)*, Florianopolis, 2016, pp. 231-234

[3] A. M. H. S. Abeykoon and K. Ohnishi, "Traction force improvement of a two-wheel mobile manipulator by changing the centre of gravity," *INDIN '05. 2005 3rd IEEE International Conference on Industrial Informatics, 2005.*, 2005, pp. 756-760.

[4] H. Sado, S. Sakai and Y. Hori, "Road condition estimation for traction control in electric vehicle," *Industrial Electronics, 1999. ISIE '99. Proceedings of the IEEE International Symposium on*, Bled, 1999, pp. 973-978 vol.2.

[5] H. Fujimoto, T. Saito, A. Tsumasaka and T. Noguchi, "Motion control and road condition estimation of electric vehicles with two in-wheel motors," *Proceedings of the 2004 IEEE International Conference on Control Applications, 2004.*, 2004, pp. 1266-1271 Vol.2.

[6] K. Johanastrom and C. Canudas-de-Wit, "Revisiting the LuGre friction model," in *IEEE Control Systems*, vol. 28, no. 6, pp. 101-114, Dec. 2008.

[7] Y. Chen and J. Wang, "Adaptive Vehicle Speed Control With Input Injections for Longitudinal Motion Independent Road Frictional Condition Estimation," in *IEEE Transactions on Vehicular Technology*, vol. 60, no. 3, pp. 839-848, March 2011.

[8] R. Rajamani, *Vehicle dynamics and control*, 2nd ed. London: Springer, 2014.

[9] J. Wong, *Theory of ground vehicles*, 1st ed. Hoboken, NJ: John Wiley, 2008.

[10] T. Murakami, F. Yu and K. Ohnishi, "Torque sensorless control in multidegree-of-freedom manipulator," in *IEEE Transactions on Industrial Electronics*, vol. 40, no. 2, pp. 259-265, Apr 1993.